Waste Management xxx (2016) xxx–xxx

Contents lists available at ScienceDirect

Waste Management

journal homepage: www.elsevier.com/locate/wasman

Spatial and temporal characteristics of elevated temperatures in municipal solid waste landfills

Navid H. Jafari [a,*], Timothy D. Stark [b], Todd Thalhamer [c]

[a] Civil and Environmental Engineering, Louisiana State University, 3316N Patrick Taylor Hall, Baton Rouge, LA 70803, United States
[b] Civil and Environmental Engineering, University of Illinois, Urbana-Champaign, 205 N. Mathews Ave., Urbana, IL 61801, United States
[c] El Dorado Hills Fire Department and Civil Engineer, Department of Resources Recycling and Recovery, California Environmental Protection Agency, Sacramento, CA, United States

ARTICLE INFO

Article history:
Received 19 June 2016
Revised 12 October 2016
Accepted 31 October 2016
Available online xxxx

Keywords:
Landfill
Municipal solid waste
Smoldering combustion
Fire
Rapid oxidation
Temperature

ABSTRACT

Elevated temperatures in waste containment facilities can pose health, environmental, and safety risks because they generate toxic gases, pressures, leachate, and heat. In particular, MSW landfills undergo changes in behavior that typically follow a progression of indicators, e.g., elevated temperatures, changes in gas composition, elevated gas pressures, increased leachate migration, slope movement, and unusual and rapid surface settlement. This paper presents two MSW landfill case studies that show the spatial and time-lapse movements of these indicators and identify four zones that illustrate the transition of normal MSW decomposition to the region of elevated temperatures. The spatial zones are gas front, temperature front, and smoldering front. The gas wellhead temperature and the ratio of CH_4 to CO_2 are used to delineate the boundaries between normal MSW decomposition, gas front, and temperature front. The ratio of CH_4 to CO_2 and carbon monoxide concentrations along with settlement strain rates and subsurface temperatures are used to delineate the smoldering front. In addition, downhole temperatures can be used to estimate the rate of movement of elevated temperatures, which is important for isolating and containing the elevated temperature in a timely manner.

1. Introduction

Approximately 840 landfill fire incidents occurred annually in the U.S. from 2004 to 2010, where >25% were repeat incidents at a specific site (Powell et al., 2016). These reoccurring incidents support observations that landfill fires are difficult to fully control, thus presenting a significant threat to the environment by releasing pungent odors (reduced sulfur compounds and organic acids), volatile organic compounds, benzene, and particulate matter (Nammari et al., 2004; Ruokojarvi et al., 1995; Lonnermark et al., 2008; Chrysikou et al., 2008). In addition, they can impact the integrity of the cover and liner systems, degrade leachate quality and gas composition, and induce slope instability and excessive settlement (Lewicki, 1999; Jafari et al., 2014; Stark et al., 2012; Øygard et al., 2005).

Powell et al. (2016) use the terms fire and subsurface exothermic events to define the incidents that affect landfill gas collection and emissions. Due to the complex nature of landfills, this paper uses elevated landfill temperature events (ETLEs) because of the many initiation mechanisms, the wide range of depth and spatial extents, and the degree of damage to landfill infrastructure and impact to the community and environment. Under this broader classification, ETLEs can represent the severity or degree of elevated temperatures, e.g., amphoteric reaction of aluminum to subsurface smoldering and pyrolysis. ETLEs can occur near the surface as fires (flaming combustion) and in the subsurface (depths >20 m) as oxygen-starved exothermic reactions. They can start locally at a gas extraction well and gradually spread to affect an entire landfill facility. Surface events generally last short durations (several hours and days), while subsurface events can last multiple years to over a decade.

Prior to the initiation of ETLEs, the in situ temperature of municipal solid waste (MSW) landfills ranges from 30 to 65 °C as a result of anaerobic decomposition. The corresponding landfill gas is composed mostly of methane (CH_4 = 45–60% v/v) and carbon dioxide (CO_2 = 40–60% v/v) in approximately equal amounts, with <3% v/v nitrogen (N_2), <1.5% v/v oxygen (O_2), <1% v/v hydrogen (H_2), and trace concentrations of carbon monoxide (CO <20 ppmv) (Martin et al., 2013; ATSDR, 2001). MSW landfills under anaerobic biodegradation typically exhibit pressures less than 5 kPa (Bogner et al., 1988; Kjeldsen and Fischer, 1995; Arigala et al., 1995), but higher gas pressures (7–16 kPa) have been estimated from inverse

* Corresponding author.
E-mail addresses: njafari@lsu.edu (N.H. Jafari), tstark@illinois.edu (T.D. Stark), ltfire88@gmail.com (T. Thalhamer).

http://dx.doi.org/10.1016/j.wasman.2016.10.052
0956-053X/

Please cite this article in press as: Jafari, N.H., et al. Spatial and temporal characteristics of elevated temperatures in municipal solid waste landfills. Waste Management (2016), http://dx.doi.org/10.1016/j.wasman.2016.10.052

analyses of landfill veneer slides caused by gas pressure build-up from leachate recirculation under composite cover systems (Thiel, 1999; Benson et al., 2012). While landfill settlement for anaerobic and enhanced (bioreactor/leachate recirculation) biodegradation is site-specific and varies significantly, field-scale studies indicate that anaerobic and enhanced biodegradation result in approximately 0.5–3%/yr and 6–16%/yr, respectively, of settlement for monitoring periods from 2 to 10.3 years and waste thicknesses of 6.8–24.3 m (Yazdani et al., 2006; Benson et al., 2007; Bareither et al., 2010; Bareither and Kwak, 2015). Table 1 presents a summary of operating conditions at MSW landfill under normal operating conditions and prior to development of ETLEs.

ETLEs are assumed herein to develop when temperatures elevate from normal conditions to above 65 °C, i.e., temperatures above which anaerobic decomposition is usually curtailed (Farquhar and Rovers, 1973; McBean et al., 1995). Factors causing ELTEs include air intrusion, partially extinguished surface fires, disposal of reactive wastes (incinerator ash, aluminum dross, and magnesium chloride), spontaneous combustion (self-heating oxidation and thermal runaway), pyrolysis and smoldering combustion. A major contributor to ETLEs is the introduction of ambient air into a landfill during gas collection and control operations and/or poor interim cover maintenance. For example, approximately 870 U.S. landfills in 2010 operated an active gas collection system, with 402 or 46% reporting at least one ETLE incident between 2004 and 2010 (Powell et al., 2016). The introduction of oxygen creates aerobic conditions that can increase waste temperatures to 85 °C and higher if smoldering combustion and pyrolysis develop. Pyrolysis is the chemical decomposition of solid material (municipal solid waste) solely by heating, thus it does not involve oxidation reactions and is endothermic (Rein, 2016). Pyrolysis results in gaseous and solid (char) products; they are both susceptible to subsequent oxidation. In particular, char oxidation leads to smoldering combustion because this heterogeneous reaction occurs on the char surface. In contrast, the oxidation of pyrolysis gas (pyrolyzate) occurs in the gas phase and leads to flaming combustion (Rein, 2016). Spontaneous combustion or self-heating also leads to flaming combustion when an unstable material oxidizes and evolves heat that is retained inside the material itself because of low thermal conductivity (Gray, 2016).

Although the majority of ELTEs are small and/or easily suppressed surface events at the working face, they can develop into large-scale subsurface events that migrate through the entire facility. Based on observations from large-scale, multi-year landfill case studies, the expansion of elevated temperatures from a localized area progresses as follows: (1) decreased methane to carbon dioxide ratio with subsequent increase generation and accumulation of carbon monoxide and hydrogen gases; (2) elevated waste and gas wellhead temperatures; (3) increase in gas pressure; (4) possible increased leachate production, migration, and pressure; (5) possible slope instability; and (6) rapid surface settlement (Stark et al., 2012; Jafari et al., 2016). These indicators characterize changes in landfill behavior from normal operating conditions of anaerobic decomposition to elevated temperatures, limited methane production, and thermal waste degradation.

Identifying this landfill progression is important because landfill operators, emergency responders, consultants, and environmental agencies need a framework to demarcate the spatial temporal boundary and rate of movement to install an isolation break, i.e., a physical barrier such as a vertical cutoff wall or an air gap created by excavating waste, to reduce the potential for elevated temperatures consuming a larger portion of the facility. However, a framework that links the progression of indicators above to the spatial and temporal characteristics of elevated temperatures is lacking. As a result, this paper uses the aforementioned indicators, specifically gas composition, temperature, and settlement, to delineate the three-dimensional boundaries and monitor the spread of ETLEs with time. In particular, this paper presents two case studies to illustrate the change in gas wellhead data and movement of subsurface elevated temperatures. The first site shows trends in gas wellhead temperature, ratio of CH_4 to CO_2, and settlement strain rate. This case study illustrates a procedure for mapping ETLEs using data measured from the landfill surface. The second site provides in situ temperatures from downhole temperature arrays to evaluate the rate and direction of subsurface heat migration. The insights from both sites are incorporated into a conceptual model that classifies a MSW landfill into five zones to determine the transition from normal operating conditions to abnormal temperature region.

Table 1
Summary of MSW landfill parameters for normal conditions (from Martin et al., 2013).

MSW landfill monitoring parameters	Normal operating conditions
Gas extraction system	
Gas wellhead temperature	<65 °C[a]
Gas pressure (kPa)	Anaerobic <5[b]
	Leachate Recirculation = 7–16[c]
Methane (v/v%)	45–60[d]
Carbon dioxide (v/v%)	40–60[d]
Carbon monoxide (ppmv)	<20[d]
Hydrogen (v/v%)	<1[d]
Waste mass	
Waste temperature	30–65°C[a]
Landfill settlement	Anaerobic = 0.5–3[e]
(% of initial thickness/year)	Leachate Recirculation = 6–16[e]

[a] U.S. EPA (2006).
[b] Young (1989), Hettiarachchi et al. (2007).
[c] Benson et al. (2012), Thiel (1999).
[d] Agency for Toxic Substances and Disease Registry (2001).
[e] Yazdani et al. (2006), Benson et al. (2007), Bareither et al. (2010), Bareither and Kwak (2015).

2. Site 1 case study

Site 1 is a MSW landfill regulated under Subtitle D regulations (40 CFR Part 258). Fig. 1(a) shows the site layout and location of the impacted area in Cells 4 through 7 (see shaded region depicting elevated temperatures). These cells encompass 26.2 ha and were constructed from late 1997 to early 2001. After reaching the permitted elevations in October 2005, Cells 4 through 7 were capped with a 0.6 m thick fine-grained soil cover. A gas control and collection system was installed and consists of 82 gas wellheads, lateral headers, and a flare station. In August 2009, five gas wellheads in Cell 5 experienced temperatures above 68 °C and as high as 95 °C. Associated laboratory gas sampling from the wellheads reported carbon monoxide concentrations >1000 ppmv, with a maximum of 10,200 ppmv. The ETLE was first observed in Cell 5 and then migrated to Cells 6 and 7 over the next four years, with Cell 4 remaining unaffected. In October 2009, the facility observed tension cracks at the crest of the Cell 5 slope and a month later slope toe bulging was observed at the bottom of the Cell 5 slope. Aerial topography from October 2008 to December 2009 indicated total settlement in excess of 6 m at the slope crest and approximately 1.2 m of upward movement at the slope toe of Cell 5.

Based on regulatory orders, the facility initiated an expanded monitoring program to identify and delineate the ETLE. This monitoring program includes gas wellhead temperature, flow rate, and pressure; gas composition (CO_2, CH_4, N_2, O_2, H_2, and CO) with a portable field gas chromatograph; and stability pins (slope

Please cite this article in press as: Jafari, N.H., et al. Spatial and temporal characteristics of elevated temperatures in municipal solid waste landfills. Waste Management (2016), http://dx.doi.org/10.1016/j.wasman.2016.10.052

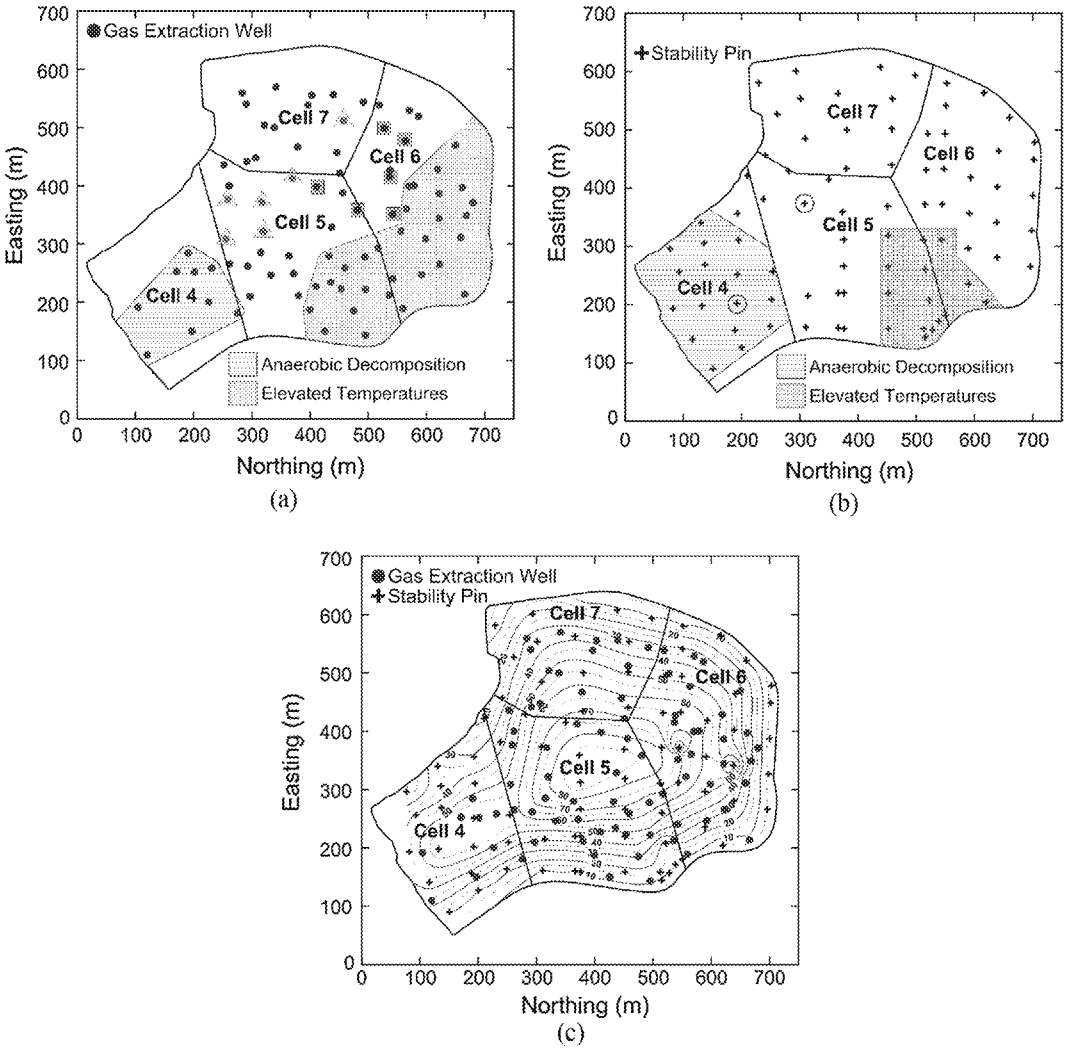

Fig. 1. Site 1 delineation of anaerobic degradation and elevated temperatures in late 2009: (a) location of gas extraction wells, (b) location of stability pins, and (c) initial waste thickness (meters).

movement and elevation) inserted below an exposed geomembrane cover system. In particular, gas temperature, flow rate, and vacuum pressure were sampled at the gas port located on the wellhead (located above the surface) and recorded using the GEM™ 2000 m (LandTec, 2010). Fig. 1(a) and (b) show the location of gas extraction wells and stability pins, respectively, used to identify landfill trends. The surface cover and bottom liner system contour elevations were used to estimate the waste thicknesses in Fig. 1(c). Vertical strains were computed as the ratio of waste thickness at a specific time divided by initial waste thickness, which was evaluated at each stability pin.

Because the landfill gas collection and removal system was operated under the New Source Performance Standards (NSPS; 40 CFR 60.753) requirements (US EPA, 1999), landfill gas temperature, flow, pressure, and composition within each wellhead were monitored monthly. This data provides an easy and routine data source to evaluate subsurface processes. The network of gas wellheads distributed across Cells 4 through 7 were used to generate plots of temperature and ratio of CH_4 to CO_2 to define the onset of elevated temperatures and spatial expansion over time. The facility installed 85 stability pins to monitor the elevation change every month. These pins were used to determine the strain rate behavior for the site and develop time-lapse plots showing locations of excessive settlement.

2.1. Gas wellhead temperatures

Fig. 2 depicts temperature contours constructed with data from 82 gas extraction wells and the kriging linear interpolation function. In addition, wellhead oxygen (O_2) levels above the NSPS limit of 5% v/v are shown in Fig. 2. Elevated temperatures at this facility began in late 2009 in 5 gas extraction wells in Cell 5 (Fig. 2(a)) and by March 2010 the facility operators observed an expanded area of gas extraction wells experiencing temperatures above 65 °C and as high as 90 °C (Fig. 2(b)). At that time, temperatures remained 30–50 °C in the unaffected cells. In September 2010, several gas wellhead temperatures in Cell 6 exhibited temperatures below 40 °C. These isolated hot spots and cooler areas indicate that some gas wellheads were experiencing elevated temperatures while the neighboring gas wellheads were reporting lower temperatures. The precipitous drop to approximately 20 °C is likely a result of air intrusion into the wellhead pipe from cracks and tears in the gas extraction well connections and cover system. This precludes air in the waste, which would result in aerobic decomposition and possible smoldering combustion. For example, Fig. 2 (c) and (d) show that high O_2 levels correspond with areas having cooler gas wellhead temperatures. In this case, O_2 levels of 15–21% v/v typically indicate the extraction well pipes and wellhead connections may be compromised. As a result, the wellhead O_2

Please cite this article in press as: Jafari, N.H., et al. Spatial and temporal characteristics of elevated temperatures in municipal solid waste landfills. Waste Management (2016), http://dx.doi.org/10.1016/j.wasman.2016.10.052

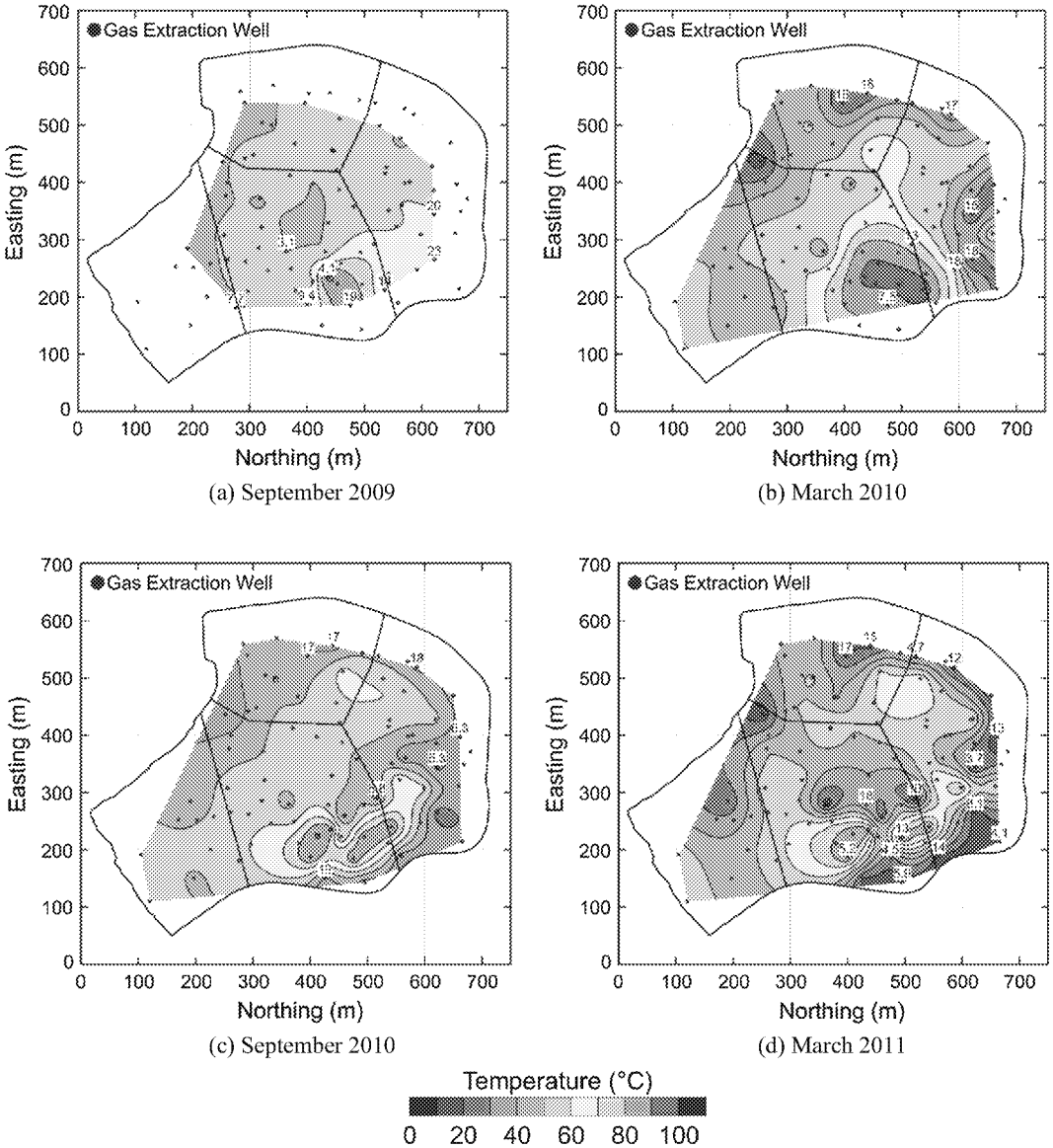

Fig. 2. Gas wellhead temperatures (°C) and O_2 levels (% v/v) in (a) September 2009, (b) March 2010, (c) September 2010, and (d) March 2011.

concentrations are similar to the ~21% v/v found in the atmosphere. However, there are instances where elevated O_2 concentrations (>5% v/v) are also observed within the region of elevated temperatures (Fig. 2(a)). These O_2 levels could indicate that air is infiltrating into the waste mass and stimulating aerobic processes and/or smoldering combustion. As a result, wellhead temperatures should be corroborated with O_2 levels to understand if air intrusion is a factor.

Cells 4–7 gas extraction wells were installed to depths of 15–40 m, with an average of 24 m. The average waste thickness across Cells 4–7 is 50 m and approximately 80 m in the center of Cell 5. A comparison of waste thickness and gas well depth indicates that the extraction wells extend only a third to half of the waste thickness. Thus, wellhead temperatures and gas composition may not represent all of the internal landfill processes along the entire waste column. For example, gas wellhead temperatures were found to underestimate waste temperatures by 10 °C to 20 °C (Martin et al., 2013; Jafari et al., 2016). Fig. 2 shows that wellhead temperatures above 65 °C can be the first signal of elevated temperatures and contour plots can be used to project the growing boundary.

2.2. Ratio of CH_4 to CO_2

Landfill gas is composed mostly of CH_4 (45–60% v/v) and CO_2 (40–60% v/v), so a ratio of CH_4 to CO_2 close to unity provides a useful measure of degree of normal anaerobic decomposition (Martin et al., 2013; Barlaz et al., 2010; Powell et al., 2006). Fig. 3 presents contours of the ratio of CH_4 to CO_2 concentration developed using average monthly values of CH_4 and CO_2 from each gas wellhead. In January 2010, almost 1.5 years after elevated temperatures were first observed, Fig. 3(a) shows the ratio of CH_4 to CO_2 remains at or above unity in Cells 4 and 7. In the elevated temperature region (Cells 5 and 6), the ratio rapidly decreases to values below 0.6, indicating CO_2 generating processes are increased. This area encompassing Cells 5 and 6 also corresponds to the shaded region in Fig. 1(a), which demarcates the gas wellheads that showed ratios of CH_4 to CO_2 below 0.6 in late 2009. The area denoting increased CO_2 production expanded in September 2010 (Fig. 3(b)) and April 2011 (Fig. 3(c)) to engulf Cells 5 and 6. The elevated temperatures continued to expand into Cell 7 by April 2011. The contours defined by ratios below 0.6 did not change from Fig. 3(c)–(d). Thus, Fig. 3 shows that anaerobic decomposition became inhibited in

Please cite this article in press as: Jafari, N.H., et al. Spatial and temporal characteristics of elevated temperatures in municipal solid waste landfills. Waste Management (2016), http://dx.doi.org/10.1016/j.wasman.2016.10.052

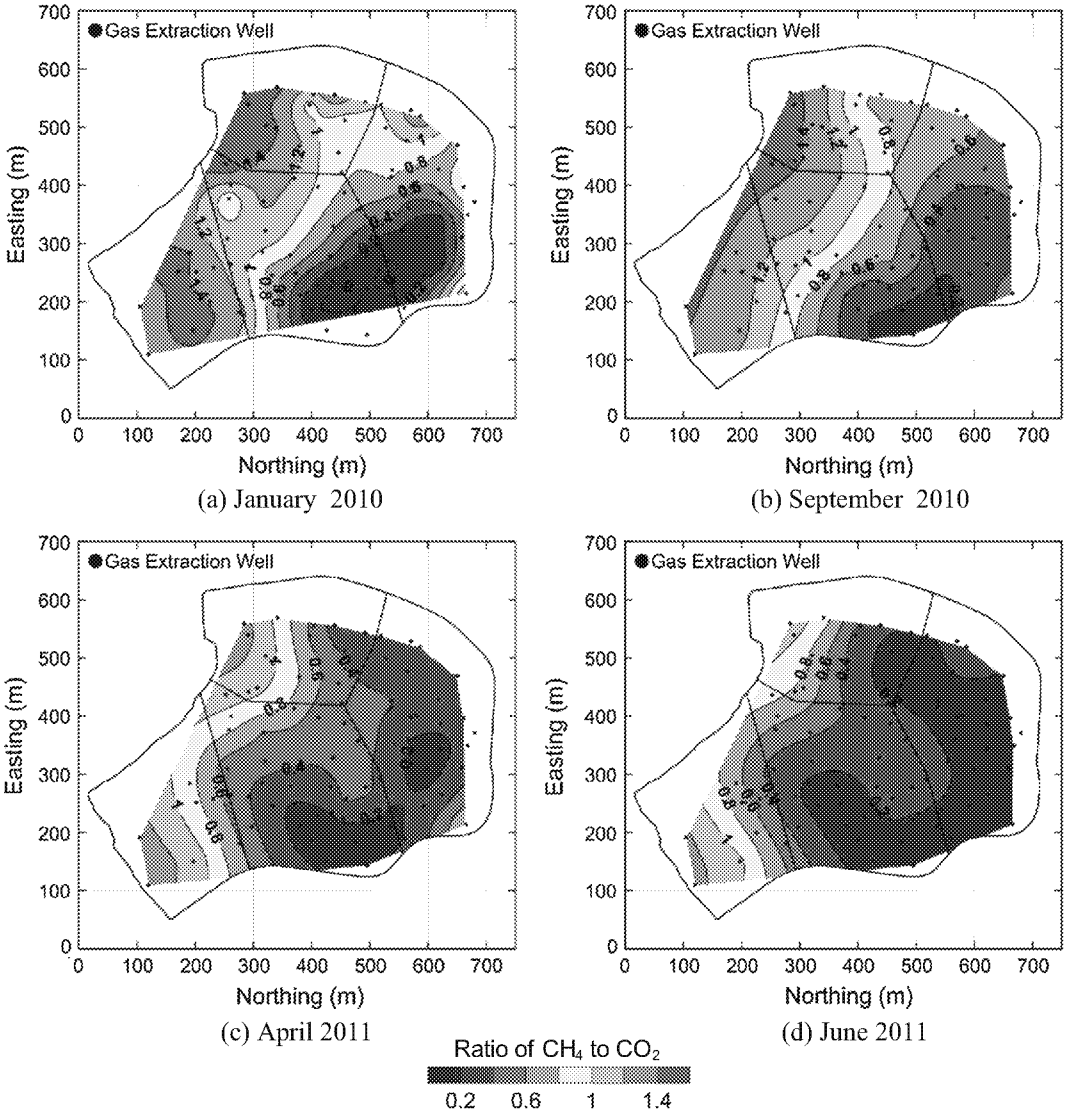

Fig. 3. Spatial expansion of decreasing gas wellhead ratio of CH_4 to CO_2 in (a) January 2010, (b) September 2010, (c) April 2011, and (d) June 2011.

Cells 5 through 7 from September 2009 to April 2011, while Cell 4 exhibited normal decomposition with ratios above unity.

In contrast to gas wellhead temperatures in Fig. 2, Fig. 3 suggests the ratio of CH_4 to CO_2 better captures the expansion of elevated temperatures. To improve the visual connection with the contours and landfill processes, ratio values below 0.6 are shaded in red to correlate elevated temperatures with reduced methane generation. On the opposite end of the spectrum, ratios greater than unity (1.0) are shaded in green, which correspond to methane production and normal operating conditions. The contours that show a decreasing trend of ratio from 1.0 to 0.6 are colored in yellow to represent a warning or hazard of elevated temperatures. Another advantage compared to wellhead temperatures is using empirical variograms in the Kriging function to describe the spatial correlation of the ratio of CH_4 to CO_2. The presence of air can decrease wellhead temperatures from approximately 50 °C to ambient air temperatures, resulting in neighboring gas wellheads to report significantly different temperatures (see Fig. 2(c)). However, the ratio of CH_4 to CO_2 is the same before and during elevated O_2 levels even though the concentrations of both gases declined.

2.3. Settlement strain rate

To calculate the settlement strain rate, the waste thickness below each stability pin prior to the start of the ETLE was determined using Fig. 1(c). The vertical strain rate (%/year) was calculated using the ratio of cumulative settlement from November 2009 divided by the initial waste thickness. Fig. 4 shows a typical trend of settlement strain rate and elapsed time for two stability pins in Cell 4 and Cell 5 (see circles in Fig. 1 (b)). The strain rate for the stability pin in Cell 4 ranges from 0.2 to 1.5%/yr, with an average of approximately 0.7%/yr. For Cell 5, the initial strain rate is similar to Cell 4 because both are experiencing mechanical and biocompression (Jafari et al., 2016). However, at an elapsed time of t = 750 days, the rate in Cell 5 increases to approximately 4%/yr by t = 900 days and continues to a peak value of 9.5%/yr at t = 1100 days. After the strain rate increases for a year, Fig. 4 shows that the strain rate gradually decreases from the peak value to ~3%/yr at t = 1600 days. The Cell 4 stability pin settles approximately 1.4 m in ~ 3.4 years (~0.5 m/yr), while the stability pin in Cell 5 subsides approximately 4.1 m in the short span of t = 750 to 1100 days (~9.2 m/yr). The behavior in Cell 5 indicates that strain rate follows normal decomposition rates until elevated

Please cite this article in press as: Jafari, N.H., et al. Spatial and temporal characteristics of elevated temperatures in municipal solid waste landfills. Waste Management (2016), http://dx.doi.org/10.1016/j.wasman.2016.10.052

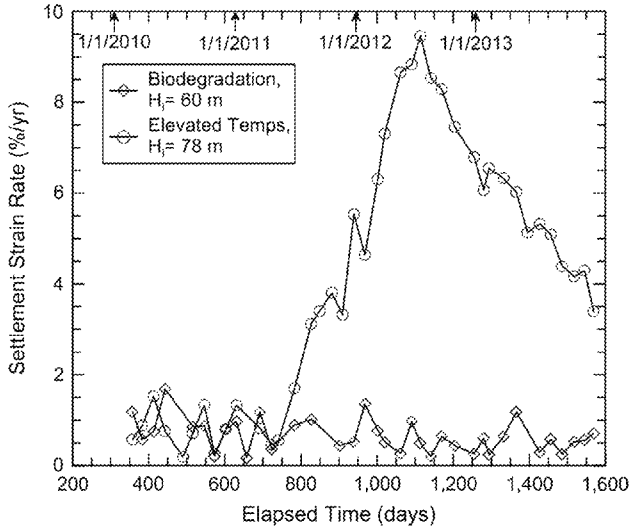

Fig. 4. Typical strain rate of normal decomposition in Cell 4 and elevated temperatures in Cell 5.

temperatures cause thermal degradation of the waste, which accelerates the strain rates. The decreasing strain rate may suggest that the thermal process is slowing down because the surrounding MSW has been consumed and/or subsurface temperatures are decreasing from insufficient heat generation.

Based on the behavior in Fig. 4, strain rates below 2%/yr suggest normal degradation settlement, i.e., mechanical and biocompression, while strain rates >3%/yr indicate elevated temperature induced subsidence. Benson et al. (2007) instrumented a 24.3 m thick landfill with settlement plates and monitored the difference in normal and bioreactor settlement rates over a 3 year period. They report areas with normal degradation experienced strain rates of approximately 1.4%/yr, whereas the bioreactor settlement plates observed an average strain rate of 4.5%/yr. In comparison to Fig. 4, the normal degradation strain rates are in agreement while the average bioreactor strain rate is greater than normal degradation but less than elevated temperatures. The bioreactor strain rate also did not exhibit a time-dependent increase in strain rate followed by a decrease, as illustrated in Fig. 4. The shaded region in Fig. 1(b) denotes the location where excessive settlement was observed during the first months of elevated temperatures and serves as a baseline for the spatial and temporal expansion of strain rate in Fig. 5. In Fig. 5(a), the area exhibiting strain rates >3%/yr is equivalent to the region exhibiting a ratio of CH_4 to CO_2 less than 0.6 (see Fig. 3(b)) and indicates that a settlement bowl or depressed area is forming. Fig. 5(a) also shows the epicenter of elevated temperatures moved between Cells 5 and 6, and the maximum strain rates within the settlement bowl are approximately 11%/yr (~7 m/yr). In October 2011, the accelerated strain rates form an arc that extends from Cell 5, boundary of Cell 7, and into Cell 6. Fig. 5(b) indicates the strain rates in Cell 5 (see northing and easting of 500 m and 200 m, respectively) are less than 3%/yr in October 2011, which was also observed in Fig. 4. These lower strain rates still represent elevated temperatures areas even though the strain rates may be more attributable to anaerobic biodegradation. The strain rates in May 2012 (Fig. 5(c)) are located in the center of Cell 5 and 6, where the waste thickness is approximately 80–90 m, and maximum strain rates are above 10%/yr. From November 2012 to October 2013, the strain rates are decreasing with time, particularly in Cell 5 where strain rates are below 2%/yr. Fig. 4 shows decreasing strain rates after a peak strain rate, so similar time-dependent settlement behavior is also occurring in Cells 4 and 5. By October 2013, accelerated strain rates are found in localized areas in Cells 6 and 7, and the strain rates remained below 2%/yr in Cell 4, which indicates waste consumption was limited in Cell 4.

Neighboring stability pins were found to exhibit similar settlement behavior, which suggests the contours in Fig. 5 are spatially correlated. An empirical variogram was applied to the kriging interpolation function to generate the smooth interpolation between stability pins in Fig. 5. For example, strain rates >4%/yr correspond to the red color to illustrate elevated temperatures, whereas strain rates less than 2%/yr are analogous to normal operating conditions and are represented by the color green.[1] The yellow and orange colors signify strain rates are increasing and suggest elevated temperatures have impacted the landfill area. The strain rates in Fig. 5 in combination with visual classification provide insight into the landfill areas experiencing significant thermal degradation of waste from elevated temperatures.

2.4. Summary of site 1

By comparing the contour plots in Figs. 2, 3 and 5, gas wellhead temperatures provide an initial boundary of elevated temperatures but they are prone to inconsistencies from possible air intrusion. In contrast, Figs. 3 and 5 show that the ratio of CH_4 and CO_2 and settlement strain rate can capture the spatial migration of elevated temperature events. A visual comparison between similar reported months shows that the region where the ratio of CH_4 to CO_2 is below 0.6 corresponds to areas of strain rates >3%/yr. Therefore, the ratio of CH_4 to CO_2 and strain rate contours were combined to develop Fig. 6. The ratio of CH_4 to CO_2 of 1.0–0.6 were chosen because they represent the increase in CO_2 generating processes. The strain rates of -3 and -4%/yr were selected based on a comparisons between Cell 4 (decomposition) and 5 (thermal degradation) strain rates. Fig. 6(a) and (b) show contours from September and October 2010, respectively. The trends in both figures indicate that limited movement of the elevated temperatures occurred between the two months. When comparing to the area of impact in Fig. 1(a), the ratio of CH_4 to CO_2 initially followed the perimeter of Cells 5 and 6. However, the ratio contours in Fig. 6(a) progressed into the center of the landfill. The same observation is found for the settlement strain rates. For example, Fig. 1(b) shows the shaded area where elevated temperature strain rates were present at the time settlement monitoring was initiated. In Fig. 6(b), this boundary moved further into the center of the landfill. The gas ratio and strain rate contours expand at different rates in Fig. 6(c) and (d). The gas ratio contours migrate into Cell 4 and a portion of Cell 7. However, the strain rate contours progress only to the center of Cells 5 and 6 in Fig. 6(c), with the strain rate contour first extending into Cell 7 in October 2011. The important observation from Fig. 6 is the increase in settlement strain rate significantly lags behind the decrease in ratio of CH_4 of CO_2, so settlement rate is not an acceptable parameter for identifying the location of the elevated temperatures and determining where an isolation break should be installed.

In summary, this case study shows that contour plots of the ratio of CH_4 of CO_2 and strain rates are useful tools to visualize the spatial and temporal expansion of elevated temperatures in an MSW facility. Specifically, Fig. 6 corroborates that decreasing ratios of CH_4 of CO_2 significantly precede accelerated strain rates, which is shown by the space between the two contours lines in Fig. 6(c) and (d). This observation suggests the decrease in gas ratio may be due to increasing waste temperatures affecting methano-

[1] For interpretation of color in Figs. 5 and 11, the reader is referred to the web version of this article.

Please cite this article in press as: Jafari, N.H., et al. Spatial and temporal characteristics of elevated temperatures in municipal solid waste landfills. Waste Management (2016), http://dx.doi.org/10.1016/j.wasman.2016.10.052

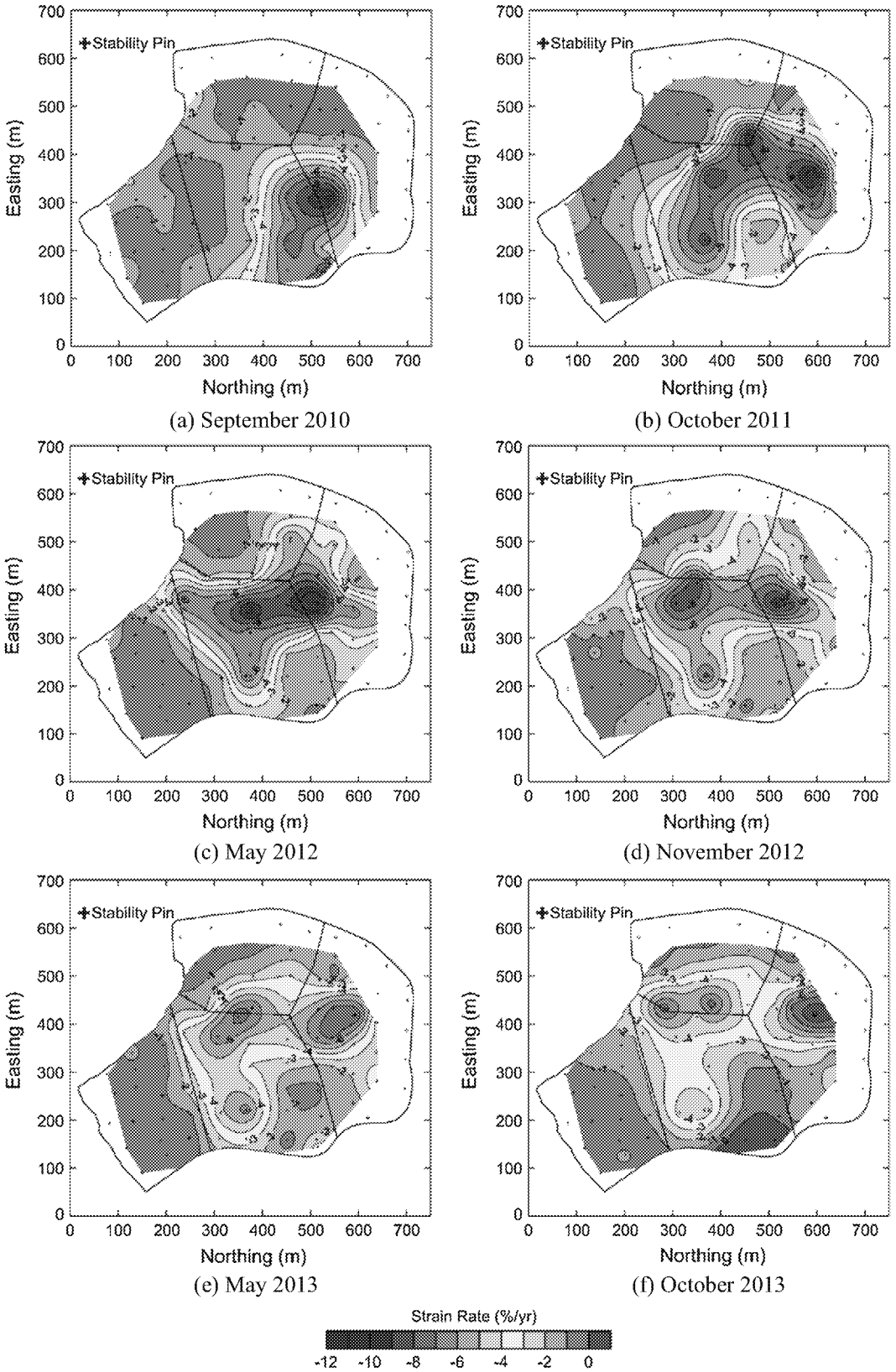

Fig. 5. Spatial and temporal movement of strain rates (%/yr): (a) September 2010, (b) October 2011, (c) May 2012, (d) November 2012, (e) May 2013, and (f) October 2013.

genesis and gas generated in the epicenter of elevated temperatures flowing to unaffected areas. The settlement strain rates in Figs. 5 and 6 also provide a method to delineate the boundary of thermal degradation of waste.

3. Site 2 case study

Site 2 landfill was originally operated as a limestone quarry from 1939 until 1988. In 1974, landfilling began in the north

Please cite this article in press as: Jafari, N.H., et al. Spatial and temporal characteristics of elevated temperatures in municipal solid waste landfills. Waste Management (2016), http://dx.doi.org/10.1016/j.wasman.2016.10.052

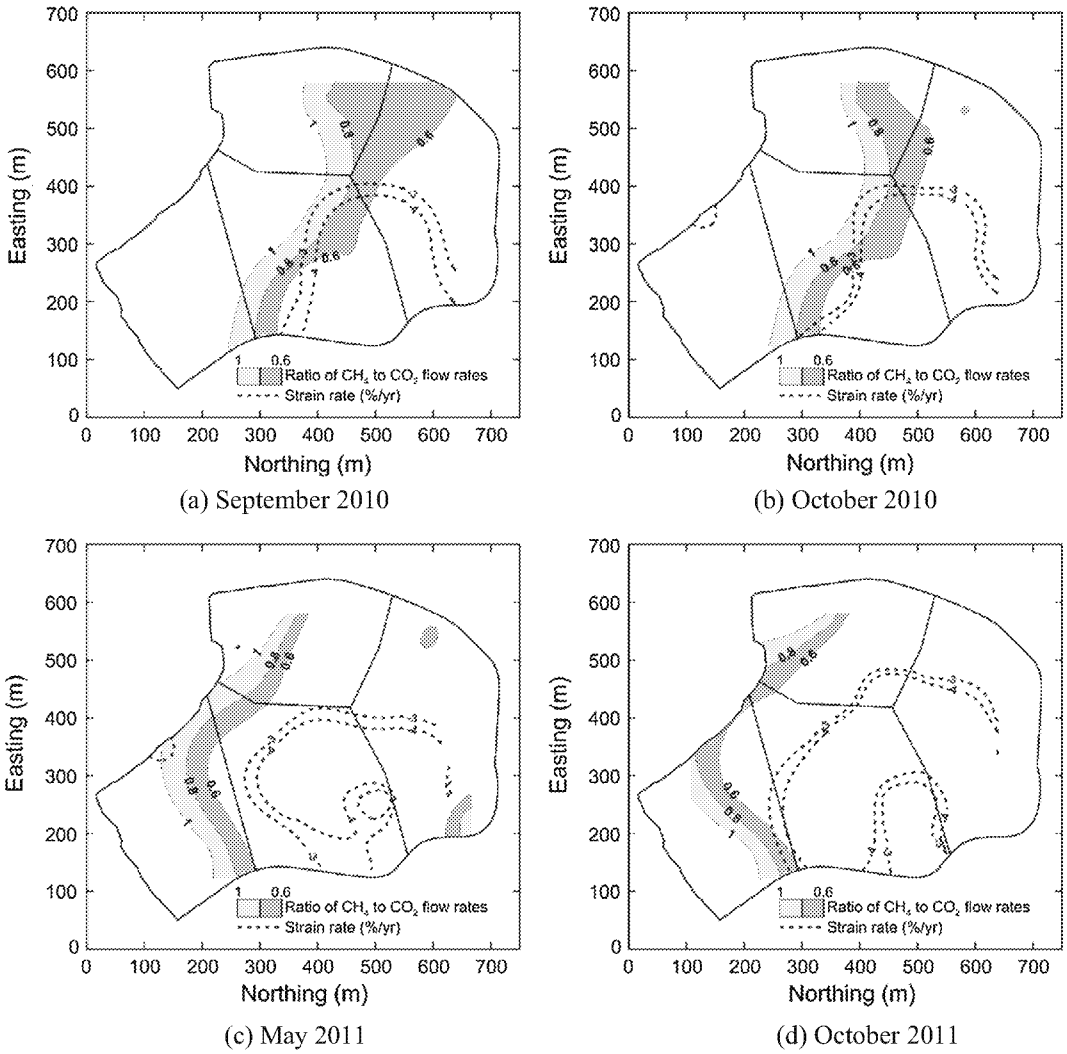

Fig. 6. Combined movement of ratio of CH_4 to CO_2 and settlement strain rate (%/yr): (a) September 2010, (b) October 2010, (c) May 2011, and (d) October 2011.

section of the quarry and continued until 1985 when the landfill underwent expansion to the southwestern areas (see Fig. 7). In August 2005, the facility stopped receiving waste and initiated closure and post-closure activities. The landfill covers an area of approximately 22.3 ha (52 acres), and extends a maximum of ~73 m below ground surface, with a total waste thickness of ~98 m. The landfill accepted approximately 13 million m^3 of waste, including commercial, industrial, and MSW, and was constructed without bottom or sideslope liner systems. The final cover system consisted of 0.6 m of compacted low hydraulic conductivity soil and 0.3 m of soil for vegetation. Leachate was collected by pumping from six leachate collection risers constructed of reinforced concrete piping that reached to the base of the quarry. The landfill gas collection and control system included 85 gas extraction wells, a system of header lines, and a blower flare station.

From November to December 2010, landfill operators noticed that several landfill gas extraction wells in the southern quarry portion were experiencing elevated wellhead temperatures and changes in gas composition (see red circle in Fig. 7). By January 2011, the wellhead temperatures at two gas extraction wells exceeded ~90 °C and CH_4 levels dropped from ~50% v/v to ~1% v/v. The facility operators installed fourteen downhole temperature arrays (DTAs) in November 2012 to monitor the magnitude and movement of subsurface elevated temperatures from the southern to northern end of the landfill (locations are shown in Fig. 7 inset). Downhole temperature arrays were installed because they provide five important pieces of information to evaluate internal landfill processes with time: (1) validate the wellhead gas composition and determine if methane generation is the dominant landfill process; (2) allow comparison between subsurface and gas wellhead temperatures; (3) provide the depth and thickness of the zone experiencing elevated temperatures, which is important for determining possible isolation and containment measures, e.g., whether or not waste excavation is a possible containment technique; (4) evaluate the rate and direction of subsurface heat migration, which can be used to assess containment measures; and (5) measure temperatures near the bottom liner system components to evaluate their condition and remaining service life.

Fig. 8 shows a typical schematic of the DTA, which consists of 15.2 cm diameter vertical wells drilled using rotary sonic or auger methods. Type T thermocouples covered in a protective sheath were installed at 6.1 m spacing to the bottom of the borehole at Site 2. The thermocouples were protected in a 50.8 mm chlorinated polyvinyl chloride (CPVC) pipe for the first 6 m, which was replaced with an abrasion protection sheath for the remaining borehole depth. A rebar was added to the CPVC pipe for structural rigidity. The well casing is backfilled with cement bentonite grout

Please cite this article in press as: Jafari, N.H., et al. Spatial and temporal characteristics of elevated temperatures in municipal solid waste landfills. Waste Management (2016), http://dx.doi.org/10.1016/j.wasman.2016.10.052

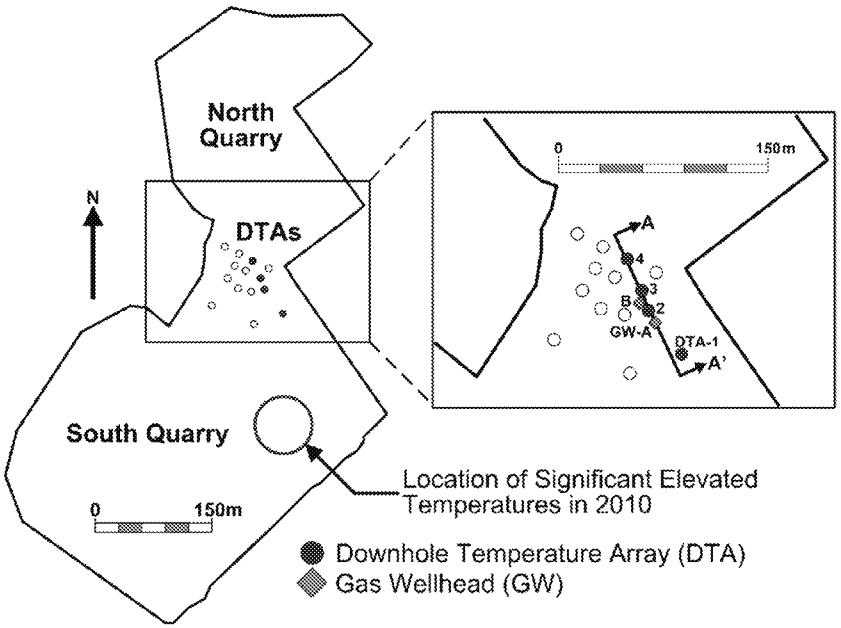

Fig. 7. Case study 2 site layout locations of DTAs with the inset showing the four DTAs used to develop cross-section A-A' and GEWs used for comparing to subsurface temperatures.

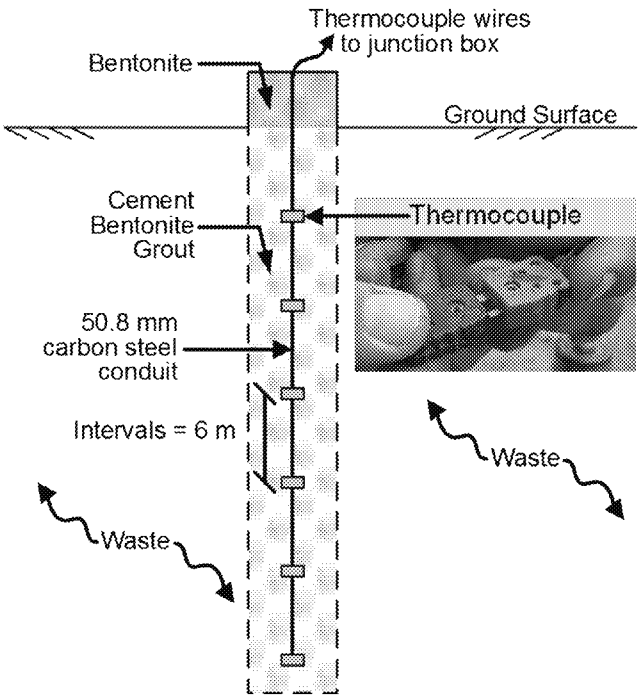

Fig. 8. Schematic of downhole temperature array with six thermocouples.

to create a consistent thermal conductivity along the well casing and prevent contact with leachate. The thermocouple wires are transferred to a junction box, where the thermocouples are recorded on a weekly basis. The Type T thermocouples are rated for a temperature range of −185 °C to 315 °C with an accuracy of ±0.5% plus 1 °C. The thermocouples were read by connecting the end clips to a Fluke 51 or an equivalent single-input thermometer. Of the 133 thermocouples installed at this facility, 30 thermocouples failed within the monitoring period from November 2012 to February 2014. Causes of thermocouple failure include high temperatures combined with wire corrosion from moisture, differential settlement, fluctuating resistance in the wires, calibration, and connectivity issues to the thermometer. With 23% of the thermocouples failing, DTAs-1 to -4 in cross-section A-A' were selected to develop the subsurface temperature contour plots because these thermocouples showed the highest survival rate (~90%). DTA-1 is also located close to the origin of elevated temperatures (see Fig. 7) so it experienced the highest subsurface temperatures as the epicenter expanded towards the DTAs.

Fig. 9 depicts waste temperatures versus elevation for cross-section A-A' depicted in the Fig. 7 inset. The cross-section utilizes four DTAs (referred to as DTA-1 through DTA-4 herein) to evaluate subsurface temperature and rates of movement. DTA-1 is the closest and DTA-4 is the farthest from the heat source, with DTA-2, DTA-3, and DTA-4 located 40 m, 55 m, and 80 m, respectively, from DTA-1. The kriging function was used to interpolate between the thermocouples and develop the temperature contours shown in Fig. 9.

After the DTAs were installed and began recording data in November 2012, the thermocouples in Fig. 9(a) measured baseline temperatures of approximately 70 °C in the center of the waste mass, with decreasing temperatures towards the ground surface and final bottom depth. This shows at the time of DTA installation the typical temperature regime prior to the ETLE. Assuming the upper boundary of anaerobic biological activity is 80 °C (Lefebvre et al. 2000; Merz 1969; Hartz et al. 1982; Mata-Alvarez and Martinez-Viturtia 1986; Pfeffer 1974), the 80 °C temperature contour can be used to delineate the front boundary of elevated temperature. The 80 °C contour was first observed two months after installation (Fig. 9(b)), and modest migration was observed between months two and six (see Fig. 9(c)). During month 7 (Fig. 9(d)), the 80 °C contour rapidly expanded towards DTA-2 and temperatures in the epicenter increased to approximately 110 °C. Over the next month (see Fig. 9(e)), the smoldering area became more prominent and temperatures at the mid-depth of the landfill increased to 130 °C. These temperatures were maintained through month 15 (see Fig. 9(f)). According to DTA-1, the maximum measured temperature in the hot spot area was 135 °C.

The hot spot in Fig. 9(e) and (f) encompasses approximately 40% of the total waste depth, i.e., temperatures ⩾80 °C extend from

Please cite this article in press as: Jafari, N.H., et al. Spatial and temporal characteristics of elevated temperatures in municipal solid waste landfills. Waste Management (2016), http://dx.doi.org/10.1016/j.wasman.2016.10.052

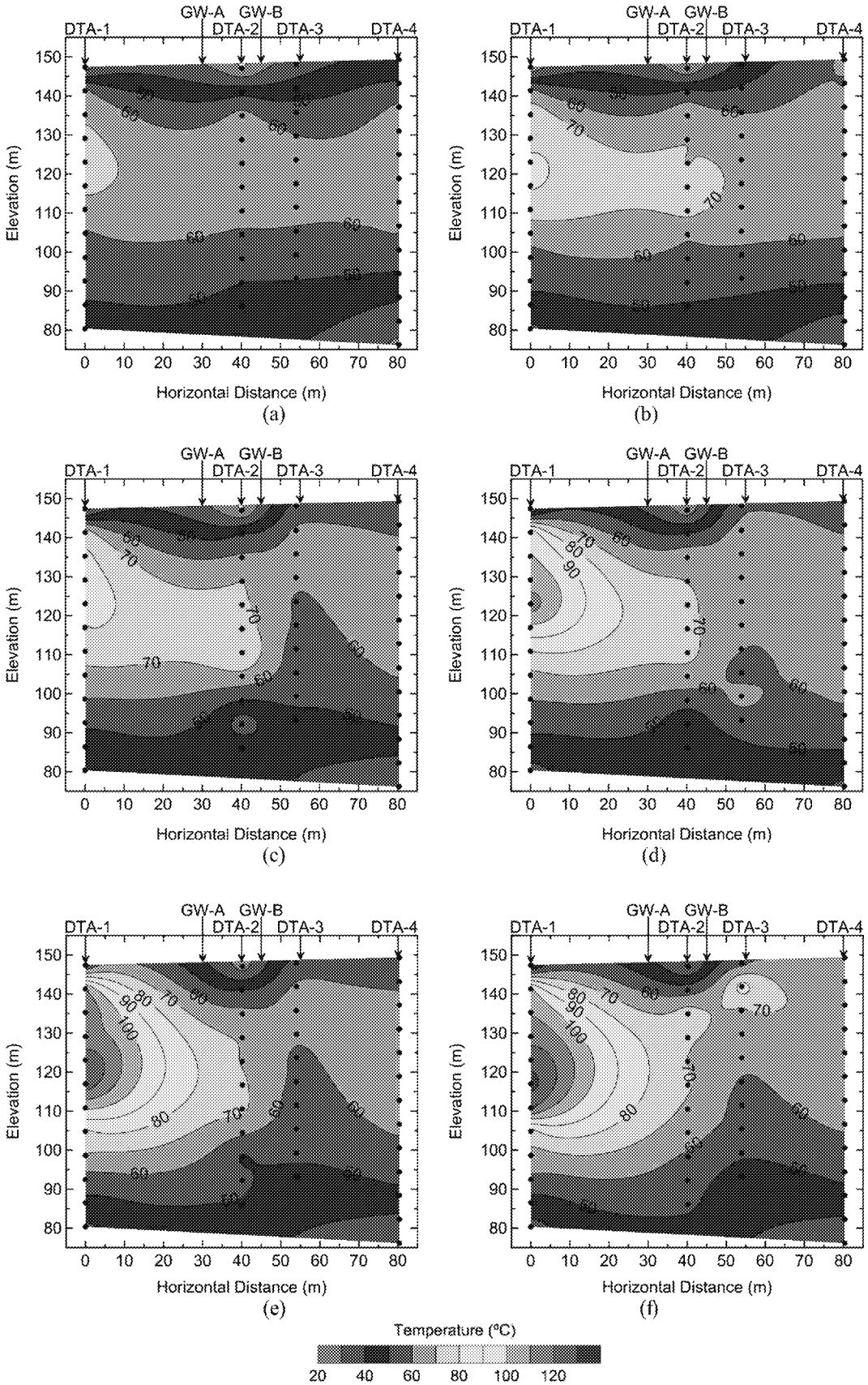

Fig. 9. Subsurface temperatures (°C) at time of (a) installation [November 2012], (b) 2 months [January 2013], (c) 6 months [May 2013], (d) 7 months [June 2013], (e) 8 months [July 2013], and (f) 15 months [January 2014].

Please cite this article in press as: Jafari, N.H., et al. Spatial and temporal characteristics of elevated temperatures in municipal solid waste landfills. Waste Management (2016), http://dx.doi.org/10.1016/j.wasman.2016.10.052

elevations of 145 m to approximately 105 m. The 80 °C contour projects towards the ground surface because of rising hot gases and elevated internal landfill pressures. Fig. 9(f) also shows an isolated event developing near the ground surface near DTA-3. This isolated area may be a result of air intrusion and eventually could daylight to the ground surface and produce flames and emit smoke into the atmosphere and/or connect to the main elevated temperature zone.

Fig. 10(a) shows temperature trends in gas extraction wells GW-A and GW-B and DTA-2. GW-A and GW-B are located approximately 30 m and 45 m from DTA-1, respectively. The maximum waste temperatures in DTA-2 are used in Fig. 10(a) to provide a comparison of wellhead temperatures as the 80 °C contour approaches. In particular, a comparison of gas wellhead and downhole temperatures indicates downhole temperatures exceed wellhead temperatures by approximately 15 °C before the ETLE approaches, which is in agreement with observations by Martin et al. (2013). During months 1 through 4, DTA-2 temperatures were 70 °C while wellhead temperatures remained at 55 °C. As the temperature of 80 °C approaches (after month 7) and eventually passes DTA-1, the gas wellhead temperatures are heated to the waste temperatures. This observation indicates that convective heat transfer is elevating the wellhead temperatures. Gas temperatures are slightly higher in GW-A than GW-B because GW-A is located closer to DTA-1 and hence is closer to the heating source. In addition, CO concentrations in GW-A (Fig. 10 (b)) are above 1500 ppmv throughout the monitoring period. The presence of CO indicates smoldering combustion and confirms that gas composition changes before elevated temperatures migrated to DTA-1. The significant drop in GW-B temperature at month 5 correlates to air intrusion because N_2 levels in GW-B increased to ~30% v/v (see Fig. 10(c)).

Downhole temperatures can also be used to estimate the rate of movement of the 80 °C contour. Quantifying the rate of movement allows landfill operators and regulatory agencies to plan a construction timeline for an isolation break or containment barrier. Using a temperature of 80 °C as a relative reference point, the change in horizontal distance of this contour in each month represents the horizontal movement rate. For example, the 80 °C contour is located 26.4 m from DTA-1 in month 7 (see Fig. 9(d)) and 30.9 m in month 8 (see Fig. 9(e)). Therefore, the temperature front moved 5 m over 1 month period. Fig. 10(d) shows the cumulative movement of the temperature front. From months 3–5 and again months 7–9, the positive rate of movement is 2.5–5 m/month. However, Fig. 10(d) shows that cumulative movement decreased from month 5 to month 6, i.e., the 80 °C contour moved backwards. This trend can be explained by air intrusion, i.e., high N_2 levels in month 5 in GW-B (see Fig. 10 (c)), which resulted in cooler waste and increased oxygen. The significant rate of movement after month six is indicative of O_2 fueled combustion, which caused the temperature front to rapidly expand laterally 15.9 m in one month. The increase in cumulative movement to approximately 30 m from month 9 to month 15 indicates the elevated temperatures did not expand significantly after month 15. In Fig. 10(a), DTA-2 corroborates this observation because temperatures peaked at 80 °C during months 5 and 6 but decreased to ~75 °C in month 7 and remained constant for the remainder of the monitoring period. Possibilities for the impeded progress include lack of oxygen to propagate smoldering combustion, a layer of inert material in the waste, e.g., interim soil cover layer acting as a thermal barrier,

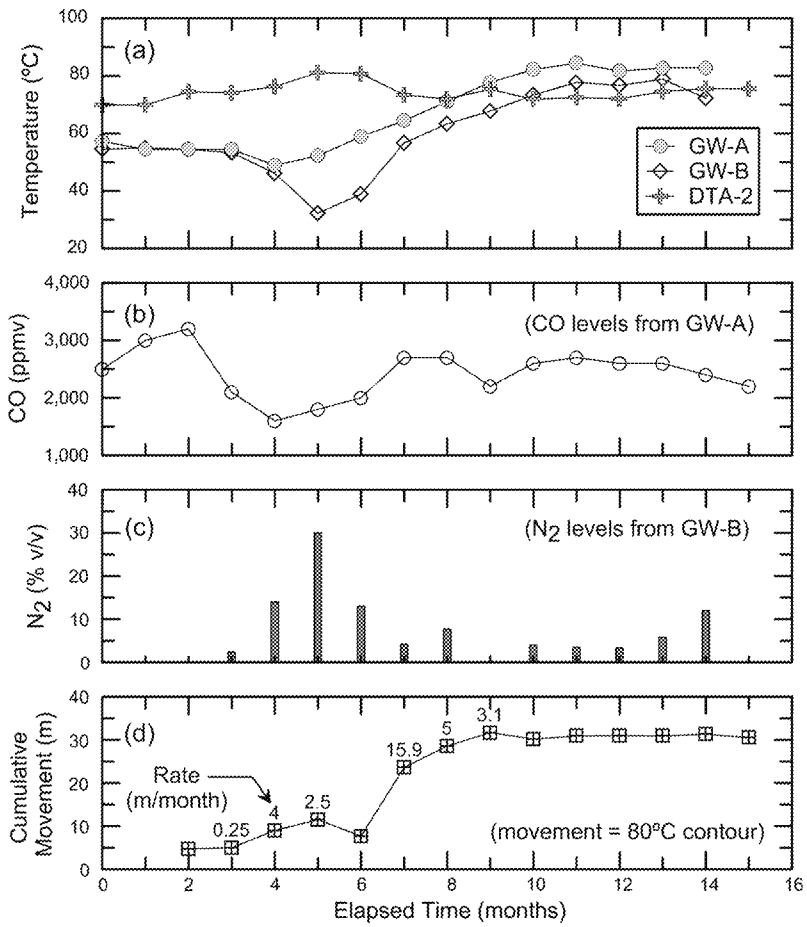

Fig. 10. Trends in (a) landfill gas wellhead and waste temperatures, (b) CO concentrations in GEW-A, (c) N_2 levels in GEW-B, and (d) cumulative subsurface movement.

Please cite this article in press as: Jafari, N.H., et al. Spatial and temporal characteristics of elevated temperatures in municipal solid waste landfills. Waste Management (2016), http://dx.doi.org/10.1016/j.wasman.2016.10.052

the elevated temperatures migrating in an alternate direction than the line of DTAs, and changes in gas management operations and interim cover system.

3.1. Summary of Site 2

The second case study shows the importance of monitoring subsurface waste temperatures, e.g., confirming wellhead gas temperatures are at least 15 °C less than subsurface waste temperatures, which may be below recognizing the occurrence of elevated temperatures. The gas wellhead temperatures are less than the subsurface temperatures due to heat loss, ambient temperature, and intermixing of gases from other areas of the landfill. The lower temperatures at DTA-2 compared to DTA-1 indicate the epicenter did not reach GWs-A or B during the monitoring period. However, as the elevated temperatures approach a gas extraction well, wellhead temperatures can increase because of convective heat transfer from gases escaping the elevated temperature region. If the ETLE reaches a gas extraction well, the gas temperatures may increase to the waste temperatures measured by the DTAs. In another case study, Martin et al. (2013) report gas wellhead temperatures are approximately 17 °C lower than waste temperatures in the ETLE epicenter. While DTA-1 measured temperatures as high as 135 °C, the maximum wellhead temperatures observed in the elevated temperature center at this site as well as Site 1 are 90–105 °C or a difference of 30–40 °C. This upper limit may be attributed to intermixing of cooler and heated gases and the vaporization of moisture from the waste, which occurs at 100 °C. As a result, it is likely that gas wellhead temperatures under predict waste temperatures before and during an elevated temperature event, with a significant increase in wellhead temperature, e.g., 10–20 °C, attributed to the approaching smoldering front.

Subsurface temperatures also identified the dominating biological and chemical processes in the waste mass. For example, the gas composition in wells GW-A and GW-B show evidence of CO concentrations >1500 ppmv, which suggests smoldering combustion is affecting gas production and composition even though temperatures at DTA-2 are approximately 75 °C and GWs-A and B are below 60 °C. This sequence of gas and temperature observations suggests that gas generated in close proximity to the epicenter is first projected in front of the ETLE and is followed by an increase in waste temperatures. Thus, Site 2 demonstrates that the ETLE spatial boundary is larger than gas wellheads experiencing ETLE indicators, which is in agreement with observations at Site 1.

The DTAs indicate the maximum recorded temperatures were 135 °C and the spatial distribution is a convex shape. Although the thermocouples in DTA-1 failed before the epicenter migrated through cross-section A-A', over 21 m of settlement in the South Quarry suggests that thermal degradation via smoldering combustion and/or pyrolysis are the dominant processes inside the landfill. The rate of movement of the epicenter was affected by air intrusion and the operation and maintenance of the gas collection system and geomembrane cover system. This observation indicates the elevated temperature region can remain stationary until air intrusion or another trigger drives smoldering combustion and expands the boundary of the event.

4. Classification of landfill zones

Evaluating the spatial and temporal variations of ETLEs requires differentiating the changes in landfill processes, e.g., anaerobic and aerobic decomposition, combustion, pyrolysis, and oxidation/reduction reactions, and the extent of these processes. The thermal degradation processes relevant in MSW landfills during elevated temperature events are smoldering combustion and pyrolysis (Martin et al., 2013; Jafari et al., 2016). Smoldering combustion is the slow, low temperature, flameless form of combustion that is sustained by heat evolved when oxygen directly attacks the surface of MSW (Kuo, 1986; Griffiths and Barnard, 1995). When organic materials are subjected to sufficient heat flux from combustion or alternative exothermic reaction under limited or no oxidation, they can degrade and gasify via the endothermic process of pyrolysis (Ohlemiller, 1995). Based on thermogravimetric analyses of MSW in N_2 gas environment, temperatures above 300 °C are required before MSW begins to thermally breakdown (Lai et al., 2012). If thermal degradation becomes the dominant pathway for landfill processes, smoldering combustion and/or pyrolysis can occur concurrently because the products of pyrolysis are oxidized in combustion. When smoldering combustion ceases because of limited oxygen supply, pyrolysis may continue for extended periods of time if sufficient heat remains. Therefore, the temperature reached during combustion and location and size of the elevated temperature epicenter within the waste mass have significant impact on the duration of the thermal degradation event.

Differentiating areas of anaerobic degradation and thermal degradation is important for emergency and environmental response and containment of these events. The landfill classification system in Fig. 11 is proposed based on the progression of indicators and the spatial and subsurface movements with time at Sites 1 and 2. Fig. 11 shows a schematic of elevated temperatures that is separated into five possible zones: (1) anaerobic decomposition, (2) gas front, (3) temperature front, (4) smoldering front, and (5) combustion/pyrolysis zone. Anaerobic decomposition is represented by temperatures below 65 °C and typical ratio of CH_4 to CO_2 greater than unity (Jafari et al., 2016). Aerobic decomposition may be present near the cracked or damaged cover system or gas wellheads and result in temperatures of 80 °C (Haug, 1997). However, anaerobic decomposition represents the baseline conditions in a landfill prior to elevated temperatures.

The gas and temperature fronts are located between anaerobic decomposition and the smoldering front and are characterized by changes to wellhead temperatures and gas composition (decreasing ratio of CH_4 and CO_2). The smoldering front follows the temperature front and is the driving force of the ETLE. Heat generated from smoldering combustion, or another exothermic reaction, can be transferred by conduction and convection to other areas of the landfill. Conduction transmits heat by direct contact between MSW particles, while convection transfers heat by movement of liquid and/or gas. In Fig. 11, the smoldering front conducts heat to the landfill waste and projects gases in advance of the ETLE. The heat generated from the smoldering front can cause pyrolysis of MSW, which yields increased gas flow and water vapor (see red arrows in Fig. 11), emits toxic and odorous gases, and cause excessive settlement. Convection forces the hot and saturated gas to rise, where it comes in contact with cooler waste material. The water vapor then condenses to leachate, which can accumulate in gas wellhead pipes, lateral headers, and develop a perched liquid level in between the ground surface and smoldering front (see Fig. 11). The leachate from condensed water vapor and dehydrated MSW can also seep toward cooler waste in the center of the landfill or gravitate to the leachate collection system. Together, the gas, temperature, and smoldering fronts are captured by the progression of indicators and can be used to delineate the location, boundary, and subsurface movement of the elevated temperature event.

The parameters used to assess the landfill zones in Fig. 11 include gas wellhead composition and temperature, subsurface temperature, and settlement. Subsurface temperatures are the most accurate because they illustrate the dimensions and migration with time and can corroborate gas compositions. The pertinent gases for evaluation of landfill zones are CH_4, CO_2, O_2, and CO. Settlement is usually monitored via topographic surveys

Please cite this article in press as: Jafari, N.H., et al. Spatial and temporal characteristics of elevated temperatures in municipal solid waste landfills. Waste Management (2016), http://dx.doi.org/10.1016/j.wasman.2016.10.052

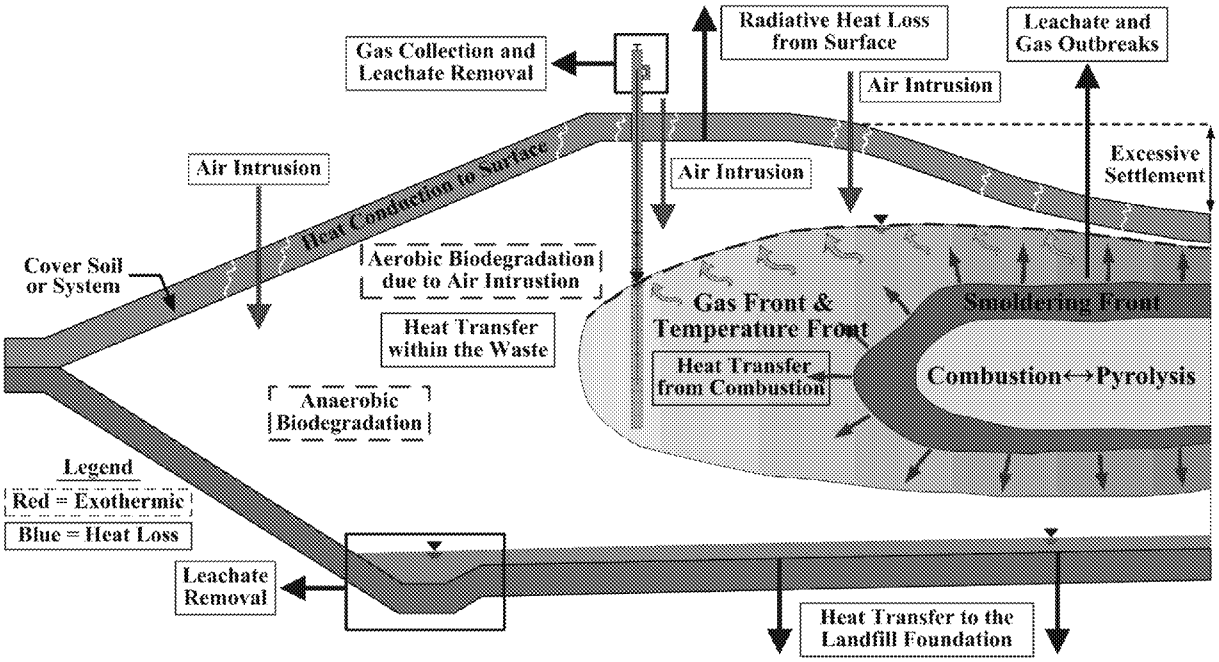

Fig. 11. Schematic of landfill zones with an elevated temperature event classified by biological and chemical processes.

and stability pins. In this instance, the exact locations should be monitored continuously to determine the change in strain rates from normal MSW decomposition to accelerated settlement.

4.1. Gas and temperature front

The criteria to determine the location of the gas and temperature fronts include the ratio of CH_4 and CO_2 because it demonstrates normal anaerobic decomposition when the ratio is greater than unity. In addition, temperature controls the quality (CH_4 and CO_2) and quantity of landfill gas generated within two temperature ranges: (1) the mesophilic range where temperatures are between 20 and 45 °C; and (2) the thermophilic range with temperatures >45–65 °C (Meima et al., 2008; Mora-Naranjo et al., 2004; ATSDR, 2001; Kotze et al., 1969). Therefore, the ratio of CH_4 to CO_2 and temperature are used in Fig. 12 to assess the location of the gas and temperature fronts.

Fig. 12 provides a compilation of CH_4 to CO_2 ratio and wellhead temperature trends for 12 gas extraction wells at Site 1. The location of the gas extraction wells used in Fig. 12 are displayed in Fig. 1(a). The purple squares and green triangles represent gas wells in Fig. 12(a) and (b), respectively. The wellheads started as normally operating wells before the smoldering front advanced towards these wells, resulting in decreasing CH_4 to CO_2 ratios with increasing wellhead temperatures. Fig. 12(a) shows a direct relationship between decreasing ratio of CH_4 to CO_2 values and increasing wellhead temperature, while Fig. 12(b) shows that the ratio of CH_4 to CO_2 decreases significantly before wellhead temperatures increase. For example, wellhead temperatures range from 40 to 55 °C in Fig. 12(a) and the gas ratio values are still above 0.8. As the ratio decreases from 0.8 to 0.1 and methane generating processes are inhibited (Kasali and Senior, 1989; Hartz et al., 1982; Pfeffer, 1974; Ahring et al., 1995), the average wellhead temperature increases from 50 to 65 °C. Wellhead temperatures continue to rise to 90 °C for ratio values less than 0.1. In contrast, Fig. 12 (b) shows that the ratio of CH_4 to CO_2 decreases from values above unity to ~0.3 before an increase in wellhead temperature is observed. Both trends in Fig. 12 indicate that the ratio of CH_4 to CO_2 is decreasing before an increase in wellhead temperature is observed. As a result, a combination of subsurface temperatures, the ratio of CH_4 to CO_2, and CO (instead of only wellhead temperatures) may be the better parameters for detecting the initiation of an ETLE because increases in wellhead temperatures can be delayed by limited heat transfer and affected by air intrusion in the wellhead. Based on the gas well locations in Fig. 1(a), it is evident that the purple squares are located near the elevated temperature shaded region, which is characterized by ratio of CH_4 to CO_2 below 0.6. This close proximity suggests that wellhead temperatures increase because heat is being transferred from the nearby smoldering front to the gas well. However, the green triangles are located farther away from the shaded region and gas composition changes before heat transfer, e.g., conduction and convection, has sufficient time to reach the gas extraction well. The appearance of CO in advance of elevated temperatures at Site 2 also corroborates the concept of a gas front. As a result, the gas and temperature front are located between normal anaerobic decomposition and the smoldering front. The temperature front is the zone adjacent to the heat source and is defined by increasing wellhead temperatures and decreasing ratio of CH_4 to CO_2. The gas front projects outward to areas unaffected by the hot spot to a greater extent than the temperature front. This region is characterized by decreasing ratio of CH_4 to CO_2 and landfill temperatures at or below the NSPS threshold of 55 °C.

4.2. Smoldering front and pyrolysis

The first indication of elevated temperatures is localized because the heat source is a discrete location or event. For example, disposing aluminum dross in a specific cell or allowing air into the waste mass via a gas extraction well or breaks in the cover system (Stark et al., 2012). The expansion of ETLEs from the original heat source signifies that smoldering combustion is present. Defining the boundary of the smoldering front is difficult because the indicator synonymous with incomplete combustion in landfills is CO, which can be found in the gas front due to gas convection (Ettala et al. 1996; Frid et al. 2010; Martin et al. 2013; Stearns and Petoyan 1984; Sperling and Henderson 2001). FEMA (2002) states that CO concentrations exceeding 1000 ppmv is indicative

Please cite this article in press as: Jafari, N.H., et al. Spatial and temporal characteristics of elevated temperatures in municipal solid waste landfills. Waste Management (2016), http://dx.doi.org/10.1016/j.wasman.2016.10.052

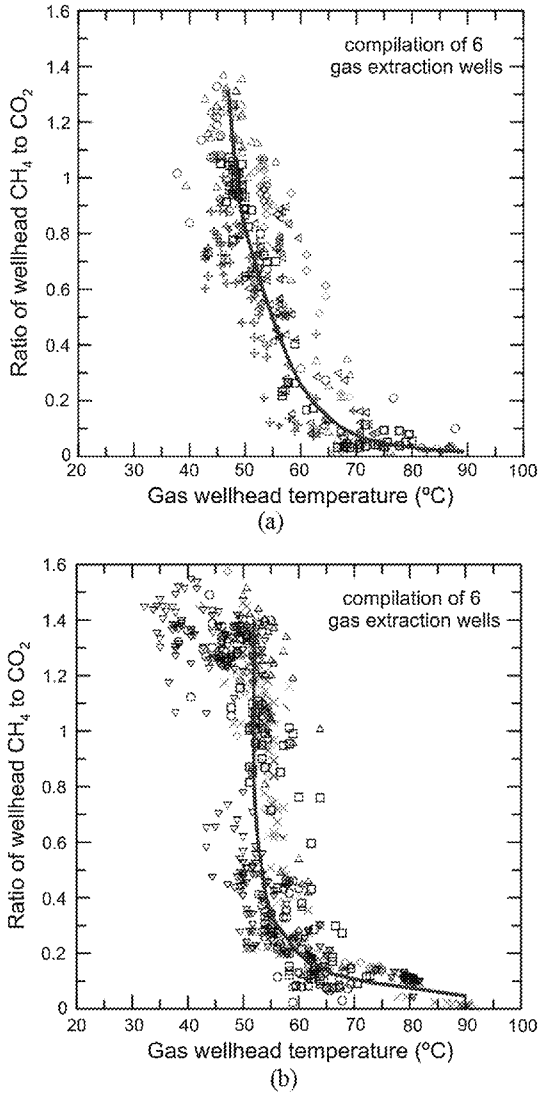

Fig. 12. Ratio of wellhead CH_4 to CO_2 as a function of wellhead temperature at Site 1: (a) temperature front and (b) gas front.

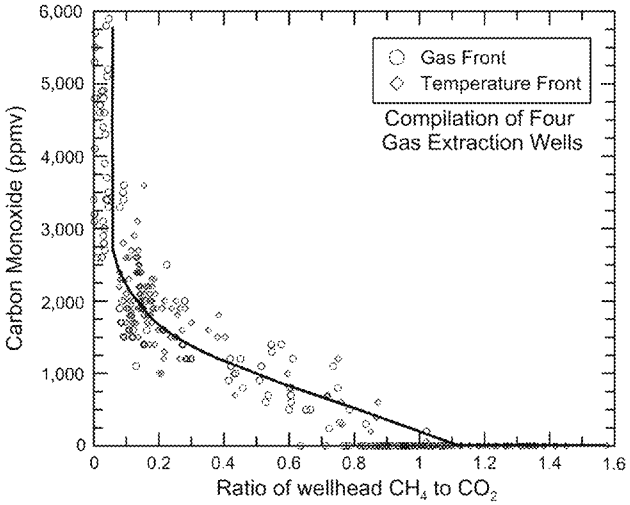

Fig. 13. Trend of ratio of CH_4 to CO_2 and CO from gas extraction wells at Site 1.

of subsurface combustion. In the proposed framework, the smoldering front is defined by CO concentrations, subsurface temperatures, and waste settlement instead of only CO concentration.

Fig. 13 shows the increasing trend of CO with decreasing ratio of CH_4 to CO_2 for four gas extraction wells found in the gas and temperature fronts in Site 1. The trend line in Fig. 13 shows an increase of CO from 0 to ~800 ppmv when the ratio of CH_4 to CO_2 decreases from 1.0–0.6. This linear trend verifies that CO is present in the gas and temperature front, with maximum concentrations reaching ~1200 ppmv. After the ratio of CH_4 to CO_2 declines to <0.2, Fig. 13 indicates that CO concentrations increase significantly, which indicate presence of the smoldering front. Martin et al. (2013) recommend CH_4 < 15% v/v and CO > 1500 ppmv to represent smoldering combustion. Based on Fig. 13, the smoldering front is defined by a ratio of CH_4 to CO_2 < 0.2 and CO > 1500 ppmv. Similar to Martin et al. (2013), a more conservative CO value of 1500 ppmv than the FEMA threshold is recommended to differentiate between CO in the temperature and combustion fronts.

In addition to the CO criterion of 1500 ppmv, subsurface temperatures and settlement are recommended to define the smoldering front. As shown in Fig. 9, subsurface temperatures >80 °C can provide an indication of the frontal boundary. Smoldering combustion may also develop at relatively low temperatures. For example, a wood member exposed to heating at temperatures as low as 77 °C for time periods ranging from several months to several years (Babrauskas, 2003) has experienced combustion, whereas the maximum temperatures measured by the DTAs at Site 2 are much higher (135 °C). Measuring subsurface temperatures indicative of smoldering combustion is difficult due to the heterogeneity of MSW composition, moisture content, insulating properties of MSW, and available oxygen in the waste mass. For example, temperatures observed in field and laboratory experiments that simulated smoldering combustion in MSW landfills range from 200 to 300 °C and as high as 700 °C (Ettala et al., 1996; Ruokojarvi et al., 1995; Lonnermark et al., 2008). Ettala et al. (1996) installed sixty-six (66) Type K thermocouples at depths of 3 and 7 m in a 180 m^3 section (10 m deep by 3 m wide and 6 m long) of a 35,000 m^3 capacity landfill, where the waste was artificially ignited in an O_2 environment of 0.7 to 3.3% v/v. Temperatures of 690 °C and 350 °C were recorded at thermocouples placed 1.5 m (depth of 7 m) and 5 m (depth 3 m) from the ignition source, respectively. However, the thermocouples located above and below these high temperature points did not show evidence of smoldering combustion, i.e., temperatures remained between 25 °C and 46 °C, which corroborates the effect of MSW heterogeneity and insulating properties. Because of the lack of spatial continuity in subsurface temperatures, a conservative DTA temperature of 80 °C was assumed to represent smoldering combustion. With this temperature threshold, a line of DTAs can be used to draw a cross-section and map the frontal boundary of smoldering combustion with CO greater than or equal to 1500 ppmv and a ratio of CH_4 to CO_2 < 0.2 (similar to Fig. 9).

A conservative estimate of the tail of the smoldering front can be delineated by strain rate contour plots. For example, Fig. 6 suggests the area within the 3%/yr contour in Site 1 signifies the tail of the smoldering front because the waste has been thermally degraded. Because pyrolysis is the mechanism leading to thermal breakdown of MSW, a contour plot of strain rates can delineate the transition from smoldering combustion to pyrolysis in Fig. 11. Temperature changes over time or space are also useful in differentiating between smoldering combustion and pyrolysis. Because combustion is exothermic and self-generating, increases in temperature both over time and space are indicative of combustion. Conversely, pyrolysis is endothermic so temperatures will decrease over time and heat transfer from the current boundary of the ETLE should not occur significantly because of the insulating properties of MSW.

Please cite this article in press as: Jafari, N.H., et al. Spatial and temporal characteristics of elevated temperatures in municipal solid waste landfills. Waste Management (2016), http://dx.doi.org/10.1016/j.wasman.2016.10.052

5. Summary and findings

Elevated temperature events can significantly impact the behavior and operation of a MSW landfill. If not addressed in an expedient manner, elevated temperatures can result in damage to the landfill infrastructure, i.e., gas extraction, leachate collection, and liner system, slope instability, and environmental conditions that adversely affect health and welfare of the local community. The sources of heat generation that cause elevated temperatures include aerobic decomposition, spontaneous combustion, reactive wastes, exothermic chemical reactions, and oxygen generated smoldering combustion. Operating parameters that can be used to evaluate the movement of ETLEs in MSW landfills include waste and gas temperatures; gas composition (ratio of CH_4 to CO_2 and CO> 1500 ppmv); and settlement strain rates. Sites 1 and 2 landfill show the following important points:

- Wellhead temperatures above 65 °C can be the first signal of development of an ETLE and contour plots can be used to project the growing boundary of the temperature front;
- Contour plots of the ratio of CH_4 of CO_2 and strain rates are useful tools to visualize the spatial and temporal expansion of elevated temperatures;
- Decreasing ratios of CH_4 of CO_2 precede accelerated settlement strain rates, i.e., >3%/yr, and provide a method to delineate the between smoldering combustion and pyrolysis.
- Gas wellhead temperatures under predict waste temperatures before and during an elevated temperature event by 10–20 °C;
- Gas generated in close proximity to the elevated temperature epicenter, which may indicate smoldering, is projected in front and is followed by an increase in gas wellhead temperatures; and
- Elevated temperature epicenter can remain stationary until air intrusion or another exothermic reaction accelerates smoldering combustion/pyrolysis and expands the boundary of the ETLE.

Based on Site 1 and 2 landfills, a landfill classification framework was proposed to define the spatial boundaries of internal processes occurring during an elevated temperature event. The landfill classification system consists of the following sequence and criteria:

1. Anaerobic Decomposition: Gas temperatures are below 65 °C and typical ratio of CH_4 to CO_2 are greater than or close to unity.
2. Gas Front: Decreasing ratio of CH_4 to CO_2 and gas wellhead temperatures at or below the NSPS threshold of 55 °C.
3. Temperature Front: Increasing gas wellhead temperatures and decreasing ratio of CH_4 to CO_2.
4. Smoldering Front: The front boundary of the smoldering front includes CO >1500 ppmv and ratio of CH_4 to CO_2 less than 0.2, combined with waste temperatures >80 °C. The tail of the smoldering front can be delineated by settlement strain rates >3%/yr, which signifies thermal degradation of the waste is occurring.

Acknowledgments

The contents and views in this paper are those of the authors and do not necessarily reflect those of any landfill owner/operator, homeowners, consultants, regulatory agency or personnel, or anyone else involved in case studies referenced. In particular, the contents of this paper/publication are the personal opinions of the author(s) and may not reflect the opinions, conclusions, policies or procedures of the California Environmental Protection Agency or CalRecycle.

References

Abring, B.K., 1995. Methanogensis in thermophilic biogas reactors. Antonie Leeuwenhoek 67, 91–102.

Arigala, S., Tsotsis, T., Webster, I., Yortsos, Y., Kattapuram, J., 1995. Gas generation, transport, and extraction in landfills. J. Environ. Eng. 121 (1), 33–44. http://dx.doi.org/10.1061/(ASCE)0733-9372(1995)121:1(33).

ATSDR, 2001. Chapter 2: Landfill Gas Basics. Landfill Gas Primer, an Overview for Environmental Health Professionals, pp. 3–14.

Babrauskas, V., 2003. Ignition Handbook: Principles and Applications to Fire Safety Engineering, Fire Investigation, Risk Management and Forensic Science. Fire Science Publishers; Society of Fire Protection Engineers, Issaquah WA, pp. 13–23. ISBN: 0-9728111-3-3. Chapter 2.

Barlaz, M.A., Staley, B.F., de los Reyes, F.L., 2010. Anaerobic biodegradation of solid waste. In: Mitchell, Ralph (Ed.), Environmental Microbiology. Wiley. Chapter 12.

Bareither, C.A., Benson, C.H., Barlaz, M.A., Edil, T.B., Tolaymat, T.M., 2010. Performance of North American bioreactor landfills: I. leachate hydrology and waste settlement. J. Environ. Eng. 136 (8), 824–838.

Bareither, C.A., Kwak, S., 2015. Assessment of municipal solid waste settlement models based on field-scale data analysis. Waste Manage. 42, 101–117.

Benson, C.H., Barlaz, M.A., Lane, D.T., Rawe, J.M., 2007. Practice review of five bioreactor/recirculation landfills. Waste Manage. 27, 13–29.

Benson, C.H., Edil, T.B., Wand, X., 2012. Evaluation of a final cover slide at a landfill with recirculating leachate. Geotext. Geomembr. 35, 100–106.

Bogner, J., Rose, C., Vogt, M., Gartman, D., 1988. Understanding landfill gas generation and migration. In: Proc., 11th Annual Int. Landfill Gas Symp., GRCDA (Government Refuse Collection and Disposal Association), Silver Spring, MD, pp. 225–242.

Chryssikou, L., Gemenetzia, P., Kouras, A., Manoli, E., Terzi, E., Constantin, S., 2006. Distribution of persistent organic pollutants, polycyclic aromatic hydrocarbons and trace elements in soil and vegetation following a large scale landfill fire in northern Greece. Environ. Int. 34 (2).

Ettala, M., Rahkonen, P., Rossi, E., Mangs, J., Keski-Rahkonen, O., 1996. Landfill fires in Finland. Waste Manage. Res. 14, 377–384.

Farquhar, G.J., Rovers, F.A., 1973. Gas production during refuse decomposition. Water, Air, Soil Pollut. 2 (4), 483–495.

Federal Emergency Management Agency (FEMA), 2002. Landfill Fires – Their Magnitude, Characteristics, and Mitigation. FA-225, Prepared by TriData Corporation, 1000 Wilson Boulevard, Arlington, Virginia for FEMA United States Fire Administration, National Fire Data Center.

Frid, V., Doudkinski, D., Liskevich, G., Shafran, E., Averbakh, A., Korostishevsky, N., Pobodko, L., 2010. Geophysical-geochemical investigation of fire-prone landfills. Environ. Earth Sci. 60 (4), 787–798.

Gray, B.F., 2016. Spontaneous combustion. SFPE Handbook of Fire Protection Engineering, Ed. M.J. Hurley, Chapter 20, pp. 604–632

Griffiths, J.F., Barnard, J.A., 1995. Flame and Combustion. Blackie Academic and Professional, Bishopbriggs, Glasgow, Scotland.

Hartz, K.E., Klink, R.E., Ham, R.K., 1982. Temperature effects: methane generation from landfill samples. J. Environ. Eng. 108 (EE4), 629–638.

Haug, R.T., 1997. Feedstocks, condition, and fire prevention. Biocycle 38 (4), 68–70.

Hettiarachchi, C.H., Meegoda, J.N., Tavantzis, J., Hettiarachchi, P., 2007. Numerical model to predict settlements coupled with land-fill gas pressure in bioreactor landfills. J. Hazard. Mater. 139 (3), 412–422.

Jafari, N.H., Stark, T.D., Rowe, R., 2014. Service life of HDPE geomembranes subjected to elevated temperatures. J. Hazard., Toxic, Radioact. Waste. 18 (1), 16–26.

Jafari, N.H., Stark, T.D., Thalhamer, T., 2016. Case Study: Progression of elevated temperatures in municipal solid waste landfills. J. Geotech. Geoenviron. Eng. accepted for publication.

Kasali, G.B., Senior, E., 1989. Effect of temperature and moisture on the anaerobic digestion of refuse. J. Chem. Tech. Biotechnol. 44, 31–41.

Kjeldsen, P., Fischer, E.V., 1995. Landfill gas migration – Field investigations at Skellingsted Landfill, Denmark. Waste Manage. Res. 13 (5), 467–484.

Kotze, J.P., Thiel, P.G., Hattingh, W.H.J., 1969. Characterization and control of anaerobic digestion. Water Res. 7 (3), 459–494.

Kuo, K., 1986. Principles of Combustion. John Wiley & Sons Inc, New York, USA.

Lai, Z., Ma, X., Tang, Y., Lin, H., 2012. Thermogravimetric analysis of the thermal decomposition of MSW in N_2, CO_2, and CO_2/N_2 atmospheres. Fuel Process. Technol. 102, 18–23.

LandTec, 2010. GEM™ 2000 gas analyzer and extraction monitors. Instruments Operation Manual, p. 64.

Lefebvre, X., Lanini, S., Houi, D., 2000. The role of aerobic activity on refuse temperature rise, I. Landfill experimental study. Waste Manage. Res. 18, 444–452.

Lewicki, R., 1999. Early Detection and Prevention of Landfill Fires. In: Proceedings Sardinia 99, Seventh International Waste Management and Landfill Symposium. CISA, Environmental Sanitary Engineering Centre, Cagliari, Italy.

Lonnermark, A., Blomqvist, Markland, S., 2008. Emissions from simulated deep-seated fires in domestic waste. Chemosphere 70, 629–639.

Martin, J.W., Stark, T.D., Thalhamer, T., Gerbasi-Graf, G.T., Gortner, R.E., 2013. Detection of aluminum waste reactions and associated waste fires. J. Hazard., Toxic, Rad. Waste. 17 (3), 164–174.

Please cite this article in press as: Jafari, N.H., et al. Spatial and temporal characteristics of elevated temperatures in municipal solid waste landfills. Waste Management (2016), http://dx.doi.org/10.1016/j.wasman.2016.10.052

Mata-Alvarez, J., Martinez-Viturtia, A., 1986. Laboratory simulation of municipal solid waste fermentation with leachate recycle. J. Chem. Tech. Biotechnol. 36, 547–556.

McBean, E.A., Rovers, F.A., Farquhar, G.J., 1995. Solid Waste Landfill Engineering and Design. Prentice Hall PTR, Englewood Cliffs, NJ.

Meima, J.A., Mora-Naranjo, N., Haarstrick, A., 2008. Sensitivity analysis and literature review of parameters controlling local biodegradation processes in municipal solid waste landfills. Waste Manage. 28, 904–918.

Merz, R.C., 1969. Special Studies of a Sanitary Landfill. Final Report Bureau of Solid Waste Management, Grant No. UI00518-08. Univ. of Southern California.

Mora-Naranjo, N., Meima, J.A., Haarstrick, A., Hempel, D.C., 2004. Modeling and experimental investigation of environmental influences on the acetate and methane formation in solid waste. Waste Manage. 24, 763–773.

Nammari, D., Hogland, W., Marques, M., Nimmermark, S., Moutavtchi, V., 2004. Emission from uncontrolled fire in municipal solid waste bales. Waste Manage. 24, 9–18.

Ohlemiller, T.J., 1995. Smoldering Combustion. SFPE Handbook of Fire Protection Engineering, 2nd. Ed., Bethesda, MD., 2-11, 2-171 – 2-179.

Øygard, J.K., Måge, A., Gjengedal, E., Svane, T., 2005. Effect of an uncontrolled fire and the subsequent fire fight on the chemical composition of landfill leachate. Waste Manage. 25, 712–718.

Pfeffer, J.T., 1974. Temperature effects on anaerobic fermentation of domestic refuse. Biotechnol. Bioeng. 16 (6), 771–787.

Powell, J., Jain, P., Kim, H., Townsend, T., Reinhart, D., 2006. Changes in landfill gas quality as a result of controlled air injection. Environ. Sci. Technol. 40 (3), 1029–1034.

Powell, J.T., Townsend, T.G., Zimmerman, J.B., 2016. Estimates of solid waste disposal rates and reduction targets for landfill gas emissions. Nat. Clim. Change 6 (2), 162–165.

Rein, G., 2016. Smoldering combustion. In: Hurley, M.J. (Ed.), SFPE Handbook of Fire Protection Engineering, pp. 581–603. Chapter 19.

Ruokojarvi, P., Ruuskanen, J., Ettala, M., Rahkonen, P., Tarhanen, J., 1995. Formation of polyaromatic hydrocarbons and polychlorinated organic compounds in municipal waste landfill fires. Chemosphere 31 (8), 3899–3908.

Sperling, T., Henderson, J.P., 2001. Understanding and controlling landfill fires. In: SWANA Landfill Symposium, San Diego, California.

Stark, T.D., Martin, J.W., Gerbasi, G.T., Thalhamer, T., 2012. Aluminum waste reaction indicators in an MSW landfill. J. Geotech. Geoenviron. Eng. 138 (3), 252–261.

Stearns, R.P., Petoyan, G.S., 1984. Identifying and controlling landfill sites. Waste Manage. Res. 2, 303–309.

Thiel, R., 1999. Design of gas pressure relief layer below a geomembrane cover to improve slope stability. In: Proc. Geosynthetics '99. Industrial Fabrics Association International, St. Paul, MN, pp. 235–252.

U.S. EPA, 1999. Summary of the requirements for the New Source Performance Standards and Emission Guidelines for municipal solid waste landfills. EPA-453R/96-004, Research Triangle Park, NC.

U.S. EPA., 2006. Landfill bioreactor performance: Second interim report, outer loop recycling & disposal facility, Louisville, Kentucky. EPA/600/R-07/060, Washington, DC.

Yazdani, R., Kieffer, J., Sananikone, K., Augenstein, D., 2006. Full Scale Bioreactor Landfill for Carbon Sequestration and Greenhouse Emission Control. Final Report, Award No. DE-FC26-01NT41152. U.S. Department of Energy, Washington, DC.

Young, A., 1989. Mathematical modeling of landfill gas extraction. J. Environ. Eng. 115 (6), 1073–1087.

Please cite this article in press as: Jafari, N.H., et al. Spatial and temporal characteristics of elevated temperatures in municipal solid waste landfills. Waste Management (2016), http://dx.doi.org/10.1016/j.wasman.2016.10.052